Science of Sintering, **56** (2024) 115-121

https://doi.org/10.2298/SOS220811024M

UDK: 666.3.019; 622.785; 53.086

The Influence of Strontium Content and Sintering Temperature on Monazite Stability

Miljana Mirković[1*)], Jelena Maletaškić[1], Svetlana Butulija[1], Ljubica Andjelković[2], Marija Šuljagić[2]

[1]Department of Materials, „VINČA" Institute of Nuclear Sciences - National Institute of the Republic of Serbia, University of Belgrade, Belgrade, Serbia.

[2]University of Belgrade - Institute of Chemistry, Technology and Metallurgy, Department of Chemistry, Njegoševa 12, 11000 Belgrade, Republic of Serbia.

Abstract:

This paper shows a simple way to synthesize a series of $Ce_{1-x}Sr_xPO_4$ ceramic materials using acetate solutions of Ce and Sr instead of nitrate which were used so far. For synthesis, the preparation method was used by simple mixing of acetate solutions of Ce and Sr (with NaH_2PO_4 at room temperature, and the studied compositions were $Ce_{1-x}Sr_xPO_4$ (where x = 0, 0.1, 0.2, 0.3, 0.4, 0.5). The disintegration of Sr in monazite structures in different sintering temperature ranges from 600 to 1000 °C was investigated. The X-ray diffraction was used to track the evolution of the phase composition with thermal treatment. The morphology of sintered ceramics was obtained by scanning electron microscopy and vibrational bands of selected spectra were observed using the FT-IR method. Relative geometric density of selected samples was evaluated. The most favorable conditions for obtaining high-temperature Ce, Sr phosphate-based ceramic material are reported.

***Keywords**: Monazite; Strontium; Sintering; XRD; SEM.*

1. Introduction

Monazite is a phosphate mineral and it is the major commercial source of Ce. The chemical composition of monazite is very complex and changeable since it rarely appears as pure $CePO_4$. The natural mineral commonly contains large amounts of uranium and thorium [1]. It is very durable and has a high isomorphic capacity for the incorporation of radionuclides [2], implying it is a superb alternative ceramic matrix for nuclear waste immobilization [3]. Two billion years old monazite deposits from Brazil are still stable, although containing different radionuclides [2]. The main advantage of monazite as the ceramic host is that it is a single-phase material and can include radionuclides as a solid solution in its crystal structure due to its flexible structural features [4]. In ceramic waste forms, radionuclides may occupy specific atomic positions in the structure of the constituent phase. The coordination polyhedral in structure impose specific size, charge and bonding compulsive on the radionuclides that can be incorporated into the structure [5]. So far, different types of rare earth phosphates have been prepared by diverse methods, such as wet chemical precipitation [6], high temperature solid state reactions [7], hydrothermal synthesis [8], and hot pressing [9]. Based on the similarity between the ionic radius of the alkaline earth

*) **Corresponding author:** miljanam@vinca.rs

and lanthanide ions, phosphate ceramics doped with different amounts of Sr can be interesting as potential Sr or U disposal materials [10]. Although monazite compounds loaded with Sr ions can be fabricated by the aforementioned synthetic methods, the most cost-effective and easiest method is the precipitation procedure from nitrate solutions [11,12].

Investigating the stability of strontium doped monazite structure itself under high temperature conditions, is of great importance especially if monazite is to be used as a host for strontium incorporation and removal [13–15]. The main goal was the investigation of the disintegration of Sr in monazite structure at different temperatures, to obtain the higher temperature stability of investigated solid solutions, especially with higher contents of Sr. The aim of this work was a development of a new pathway for the synthesis of $Ce_{1-x}Sr_xPO_4$ materials from acetate solutions. Several methods were applied in order to study the phase and chemical composition, thermal evaluation, and the sintering behavior of synthesized materials.

2. Materials and Experimental Procedures

All the chemicals used in the sample preparation were of p.a. grade and produced from Sigma Aldrich. Compositions of nominal formula $Ce_{1-x}Sr_xPO_4$ were obtained (where x = 0, 0.1, 0.2, 0.3, 0.4, 0.5). The calculated amounts of Ce and Sr acetate for each nominal composition were dissolved in 50 cm^3 of deionized water and mixed with 50 cm^3 NaH_2PO_4 solution at 60°C for one hour. Reactants were added in the calculated mass ratio to obtain pure monazite and monazite with mass of 10%, 20%, 30%, 40% and 50% of Sr in structure. After the precipitation reaction, the resulting precipitates were left to cool down for one hour at room temperature. The precipitates were washed with distilled water, centrifuged six times for 10 minutes at 3500 rpm, and dried at 70 °C overnight. The obtained powders were pressed in a steel mold into pellets with a diameter of 7 mm and thickness of 2 mm at 50 MPa. The density of selected sintered samples is determined in relation to theoretical density of monazite structure (5.247 g/cm^3) [9].

Sintering of compacted powders was carried out at different temperatures (from 600, 800, and 1000 °C) in a horizontal tube furnace (Protherm furnace, Turkey) under ambient atmosphere at a heating rate of 10 °C/min for 2 h in an alumina crucible. The phase stability, chemical composition, and microstructural features of sintered materials were investigated.
The phase composition of synthesized powders and sintered samples as well were examined using X-ray diffraction (Rigaku Ultima IV, Japan). The X-ray beam was nickel-filtered Cu$K\alpha_{1,2}$ radiations λ = 0.1540 nm, operating at 40 kV and 40 mA. XRD data were collected from 5° to 65° 2θ at scanning rate of 2°/min using Scintillation counter. Phase analysis was done by using PDXL2 software (version 2.0.3.0) [16], with reference to the patterns of the International Centre for Diffraction Data database (ICDD), card number which were used were: PDF Card - 01-083-0650, monazite, PDF Card - 01-087-0561, $\alpha Sr_2P_2O_7$ [17], version 2012.

Microstructure and chemical composition were investigated with Au/Pd coating using a scanning electron microscope (SEM) Vega TS 5130MM, Tescan, coupled by EDS (INCA PentaFET-x3, Oxford Instruments). Infrared spectra of the synthesized powder samples were recorded at ambient conditions between 4000-400 cm^{-1}(mid-IR region) with a Nicolet IS 50 FT-IR Spectrometer by using the ATR sampling technique.

3. Results and Discussion

XRD results of synthesized $CeSrPO_4$ are presented in Fig. 1.

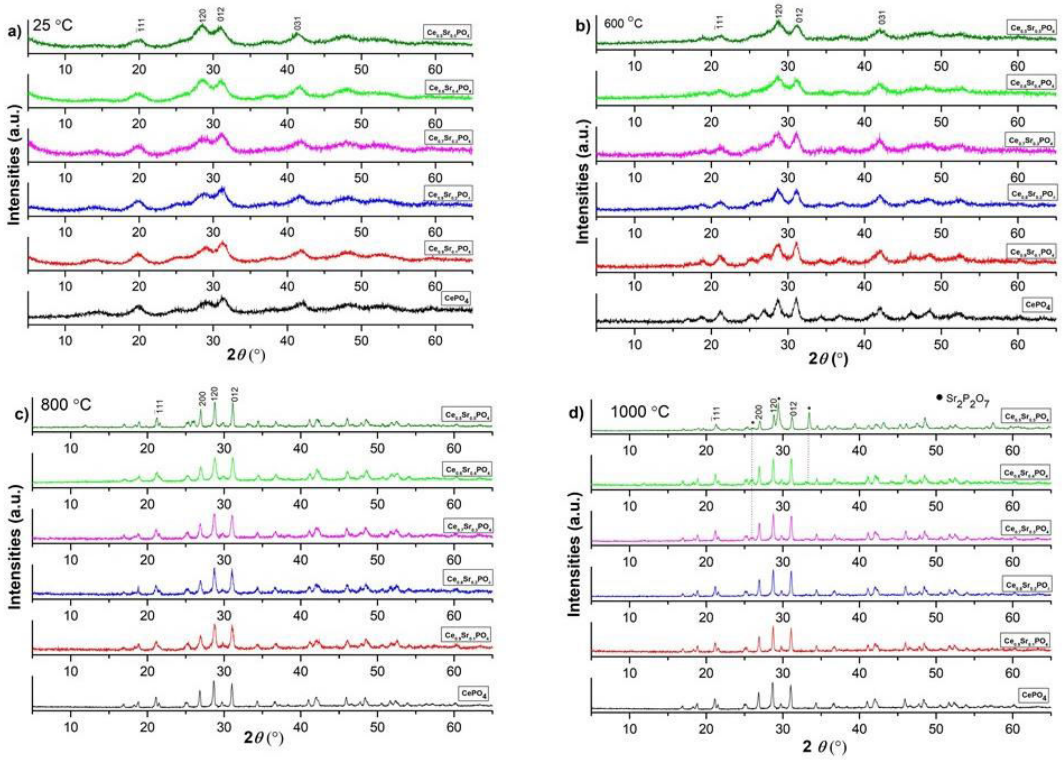

Fig. 1. XRD results of Monazite-$CePO_4$ with defined amounts of Sr in structure: $Ce_{0.9}Sr_{0.1}PO_4$, $Ce_{0.8}Sr_{0.2}PO_4$, $Ce_{0.7}Sr_{0.3}PO_4$, $Ce_{0.6}Sr_{0.4}PO_4$, and $Ce_{0.5}Sr_{0.5}PO_4$ a) as-prepared samples, b) sintered at 600 °C, 2h; c) sintered at 800 °C, 2h and c) sintered at 1000 °C, 2h.

The Monazite-type monoclinic crystal structure in $P12_1/n1$ space group was obtained. The diffractograms of as-prepared samples are shown in Fig. 1a. Double peak at about 28.7° and 31.3° 2θ presents main monazite *hkl* reflections: 120 and 012. With the increase of Sr in the structure, an increase in intensity and symmetry of reflection was observed. The peak at about 41° 2θ, corresponding to reflection 031, became more intense and sharper with the higher Sr amount in the structure. Furthermore, the slight deformation of the monazite structure occurred caused by the incorporation of Sr. This is indicated by the slight shift of the peaks to the left, Fig. 1. The powder diffractograms given in Figs 1b and 1c contains reflections of pure monazite phase, indicating the absence of contamination and secondary phases in the prepared samples.

As can be clearly seen, with the increase in sintering temperature to 600 °C, a partial arrangement of the crystal structure occurs. Somewhat more defined and sharper peaks were observed, Fig. 1b. The diffractograms for the samples sintered at 800 °C showed a much better arrangement of the crystal structure. The peaks are much sharper, narrower and with higher intensities in contrast to the peaks of the samples sintered at 600 °C. The results of the XRD analysis of the samples sintered at 1000 °C are shown in Fig. 1d. An increase in Sr content (30, 40 and 50%) in samples $Ce_{0.7}Sr_{0.3}PO_4$, $Ce_{0.6}Sr_{0.4}PO_4$ and $Ce_{0.5}Sr_{0.5}PO_4$ led to the separation of the distrontium diphosphate secondary phase (α-$Sr_2P_2O_7$, marked by a black

circle in Fig. 1d), indicating that the monazite structure remains stable at 1000 °C only with the addition of 10% and 20% of Sr (samples: $Ce_{0.9}Sr_{0.1}PO_4$ and $Ce_{0.8}Sr_{0.2}PO_4$).

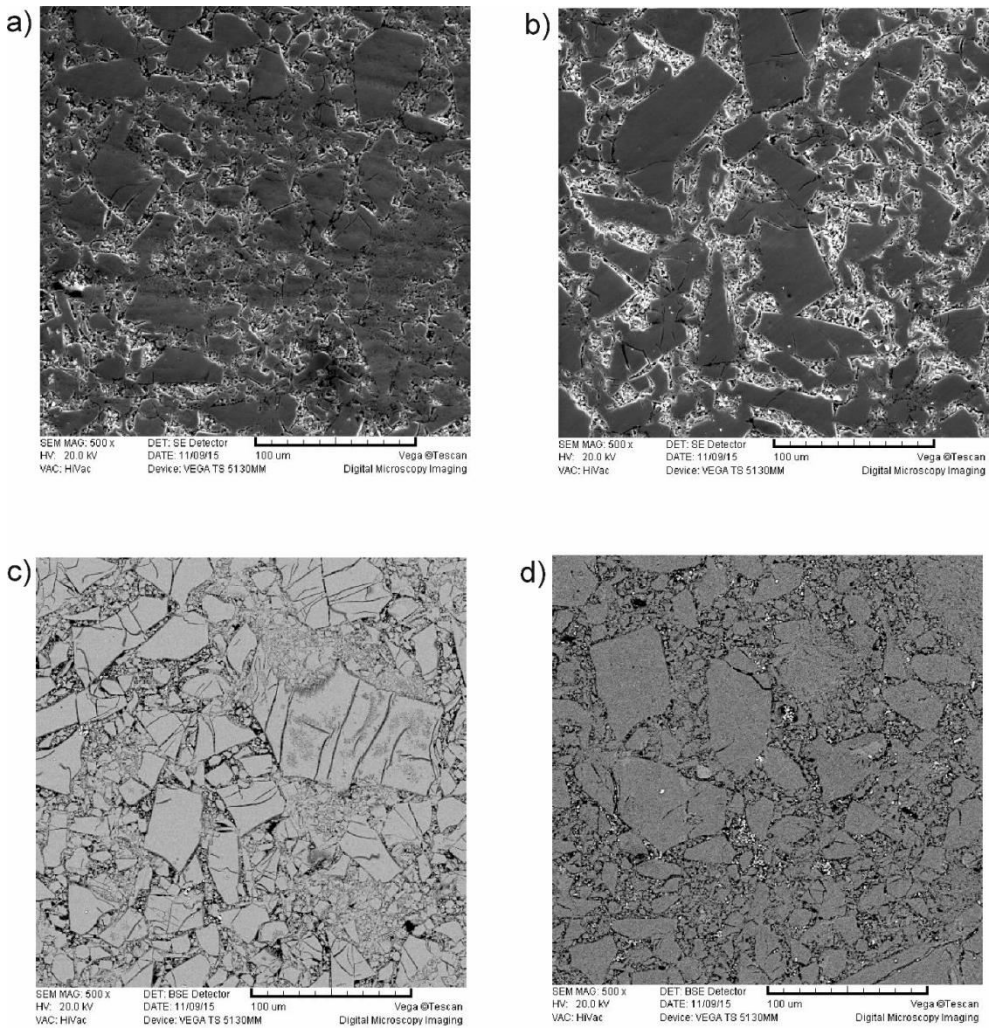

Fig. 2. SEM micrographs of a) $CePO_4$, b) $Ce_{0.9}Sr_{0.1}PO_4$, c) $Ce_{0.7}S_{r0.3}PO_4$ and d) $Ce_{0.5}Sr_{0.5}PO_4$ sintered at 1000 °C.

The morphologies of the samples sintered at 1000 °C for 2 hours have been investigated using SEM and are shown in Fig. 2. On Fig. 2a micrograph of pure $CePO_4$ monazite sintered ceramic is shown. The monazite grains have proper prismatic monoclinic appearance, with approximate sizes between 30 μm and 50 μm. Fig. 2b shows morphology of sintered $Ce_{0.9}Sr_{0.1}PO_4$ and relives some larger grains than in pure monazite, with elongated monoclinic prismatic appearance. Grains are randomly oriented in main matrix, with sizes between 50 μm and 100 μm. The morphology of sintered $Ce_{0.7}S_{r0.3}PO_4$ is shown on Fig. 2c, and it shows some larger and smaller prismatic grains that are interconnected together and forming blocks. The influence of temperature with a slightly higher mass addition of Sr leads to greater grain growth, but also to mutual compaction, creating a somewhat more homogeneous basic matrix. The smaller grains are about 20 μm in size while the larger blocks are over 100 μm in size. At Fig. 2d $Ce_{0.5}Sr_{0.5}PO_4$ sample is shown, and micrograph reveals large prismatic grains with a size of about 90 μm in length and 30 μm in width, also in the matrix slightly brighter dotted fields are observed that most likely originate from the secondary phase. In all cases, the

samples were uniform and consisted of large, compacted particles. An abundant agglomeration was presented, irrespective of Sr amount added.

FT-IR spectra of selected $Ce_{1-x}Sr_xPO_4$ for as-prepared and samples sintered at 1000 °C are presented in Fig. 3, while detailed assignments are given in Table I. The presence of lattice water and surface adsorbed water in as-prepared samples gave rise to two peaks at ≈3300 cm^{-1} and ≈1620 cm^{-1}. However, these peaks were not visible for samples sintered at 1000 °C due to water evaporation. In the case of as-prepared samples, bands at approximately 990 cm^{-1} and 930 cm^{-1} originated from asymmetric and symmetric stretching vibration modes of P-O bonds in orthophosphates. Bands at ≈ 600 cm^{-1} and ≈ 500 cm^{-1} were related to bending vibrations of P-O bonds [18–22]. Peaks of orthophosphates were also visible at spectra of sintered samples. Since the asymmetric and symmetric stretching vibration modes of terminal pyrophosphate PO_3 groups could be found in the same region [18], orthophosphates bands were overlapped with pyrophosphate bands. The weakening of the phosphate bands at about 960 cm^{-1} and 600 cm^{-1} with increase of Sr content in well-ordered sintered monazite structure were also observed.

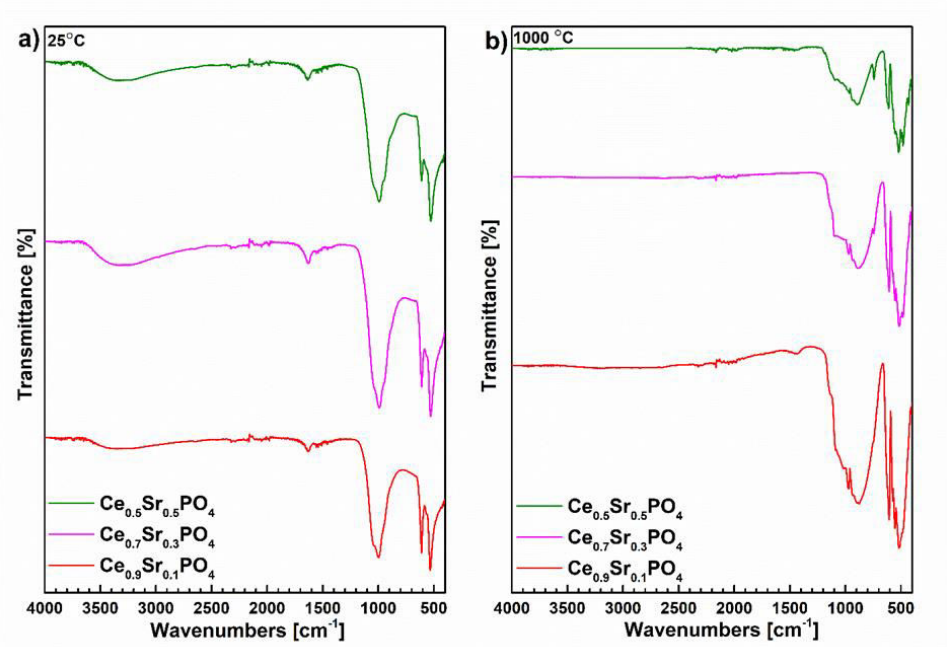

Fig. 3. FT-IR spectra of Monazite-$CePO_4$ with addition of 10% Sr, 30% Sr, and 50% Sr a) as-prepared, b) sintered at 1000 °C.

Tab. I IR assignments for Monazite-$CePO_4$ with addition of 10% Sr, 30% Sr, and 50% Sr.

Monazite	Assignments (Wavenumber, cm^{-1})					
	Orthophosphate, PO_4^{3-}		Pyrophosphate, $P_2O_7^{2-}$		Water, H_2O	
	25 °C	1000 °C	25 °C	1000 °C	25 °C	1000 °C
$Ce_{0.9}Sr_{0.1}PO_4$	996, 944 614, 530	967, 910 602, 514	---	---	3370 1625	---
$Ce_{0.7}Sr_{0.3}PO_4$	993, 937 606, 526	975, 923 599, 500	---	1102, 923	3321 1632	---
$Ce_{0.5}Sr_{0.5}PO_4$	989, 932 610, 528	976, 903 605, 507	---	1094, 910	3335 1646	---

The theoretical densities of $Ce_{0.9}Sr_{0.1}PO_4$, $Ce_{0.7}Sr_{0.3}PO_4$, $Ce_{0.5}Sr_{0.5}PO_4$ were calculated in relation to the pure theoretical density of monazite (5.247 g/cm^3). The relative density was obtained in relation to the theoretical density and amounts 80% for $Ce_{0.9}Sr_{0.1}PO_4$ (5.097 g/cm^3), 79% for $Ce_{0.7}Sr_{0.3}PO_4$ (4.865 g/cm^3), and 77% for $Ce_{0.5}Sr_{0.5}PO_4$ (4.632 g/cm^3). The theoretical density is lower as the addition of Sr in the monazite structure is higher.

4. Conclusion

The Monazite type materials with different amounts of strontium ($Ce_{1-x}Sr_xPO_4$, x=0.1, 0.2, 0.3, 0.4) were successfully synthesized by precipitation method from acetate salts and sintered at 600, 800, and 1000 °C. Better crystallinity and structure ordering with increase of strontium content and sintering temperature were observed in all samples. XRD results revealed that pure monazite structure remained stable at 1000 °C for $Ce_{0.1}Sr_{0.9}PO_4$ and $Ce_{0.2}Sr_{0.8}PO_4$, while at higher Sr concentrations separation of secondary α-$Sr_2P_2O_7$ phase occurred. The addition of strontium did not affect morphology. FT-IR results were in accordance with XRD analyses, confirming the presence of secondary phase for $Ce_{0.3}Sr_{0.7}PO_4$ and $Ce_{0.5}Sr_{0.5}PO_4$ sintered at 1000 °C. The theoretical density decrease with increase of strontium in monazite structure, where in our case it can be explained that there is a disturbance of the density due to the separation of the secondary pyrophosphate phase in samples with a strontium content higher than 20% in the monazite structure. The obtained results indicate that such material might be successfully potentially used as a thermally stable and cost effective matrix for nuclear waste immobilization.

Acknowledgments

The authors would like to special thank dr Violeta Nikolić, for FT-IR experimental measurements of samples. The authors would like to thank the Ministry of Education, Science and Technological Development of Republic of Serbia (Grant Nos. 451-03-68/2022-14/200017, within the topic number: 1702202, and 451-03-68/2022-14/200026) for financial support.

5. References

1. N. Clavier, R. Podor, N. Dacheux, J. Eur. Ceram. Soc. 31 (2011) 941.
2. M.I. Ojovan, W.E. Lee, 18 - New Immobilising Hosts and Technologies, in: M.I. Ojovan, W.E. Lee (Eds.), An Introd. to Nucl. Waste Immobil. Second Ed., Elsevier, Oxford, 2014: pp. 283–305.
3. R. Asuvathraman, K. Joseph, R. Raja Madhavan, R. Sudha, R. Krishna Prabhu, K. V Govindan Kutty, J. Eur. Ceram. Soc. 35 (2015) 4233.
4. N. Dacheux, N. Clavier, R. Podor, Am. Mineral. 98 (2013) 833.
5. R.C. Ewing, W. Lutze, Ceram. Int. 17 (1991) 287.
6. P. Chen, T.-I. Mah, J. Mater. Sci. 32 (1997) 3863.
7. K. Ravindran Nair, P. Prabhakar Rao, B. Amina, M.R. Chandran, P. Koshy, Mater. Lett. 60 (2006) 1796.
8. B. Yan, X. Xiao, Nanoscale Res. Lett. 5 (2010) 1962.
9. Y. Teng, P. Zeng, Y. Huang, L. Wu, X. Wang, J. Nucl. Mater. 465 (2015) 482.
10. S.K. Gupta, A.K. Yadav, S. Nigam, S.N. Jha, C. Mazumder, D. Bhattacharya, S.K. Thulasidas, Spectrochim. Acta Part A Mol. Biomol. Spectrosc. 151 (2015) 453.
11. T. Hernández, P. Martín, J. Alloys Compd. 466 (2008) 568.

12. E.G. del Moral, D.P. Fagg, E. Chinarro, J.C.C. Abrantes, J.R. Jurado, G.C. Mather, Ceram. Int. 35 (2009) 1481.
13. D. Rawat, S. Phapale, R. Mishra, S. Dash, Thermochim. Acta. 674 (2019) 10.
14. K.K. Ohtaki, N.J. Heravi, J.W. Leadbetter, P.E.D. Morgan, M.L. Mecartney, Solid State Ionics. 293 (2016) 44.
15. F. Wang, L. Li, H. Zhu, Q. Liao, J. Zeng, Y. Wang, K. Wu, Y. Zhu, J. Non. Cryst. Solids. 588 (2022) 121631.
16. Rigaku, PDXL Integrated X-Ray Powder Diffraction Softvare, Rigaku, Tokyo, Japan, 2011.
17. International Crystallographical Database (ICDD), in: N.S. 12 Campus Blvd, PA 19073, USA, 2012.
18. J. Demol, E. Ho, G. Senanayake, Hydrometallurgy. 179 (2018) 254.
19. J. Heuser, A.A. Bukaemskiy, S. Neumeier, A. Neumann, D. Bosbach, Prog. Nucl. Energy. 72 (2014) 149.
20. T. Masui, H. Tategaki, S. Furukawa, N. Imanaka, J. Ceram. Soc. Japan. 112 (2004) 646.
21. D. Đukić, M. Šuljagić, L. Andjelković, V. Pavlović, D. Bučevac, B. Vrbica, M. Mirković, Sci. Sinter. 54, 3 (2022) 287.
22. T. V. Maksimović, J.P. Maksimović, P.I. Tančić, N.I. Potkonjak, Z.P. Nedić, L.G. Joksović, M.C. Pagnacco, Sci. Sinter. 53, 2 (2021) 223.

Сажетак: *У овом раду је приказан једноставан начин да се синтетише серија* $Ce_{1-x}Sr_xPO_4$ *керамичких материјала коришћењем ацетатних раствора Ce и Sr уместо до сада коришћених нитрата. За синтезу је коришћен метод припреме једноставним мешањем раствора* $Ce(C_2H_3O_2)_3{\cdot}xH_2O$*),* $Sr(C_2H_3O_2)_2$*, и* NaH_2PO_4 *као прекурсора на собној температури, а испитивани састави су* $Ce_{1-x}Sr_xPO_4$ *(где је к = 0 , 0,1, 0,2, 0,3, 0,4, 0,5). Испитивана је дезинтеграција Sr у структурама моназита у различитим температурним распонима синтеровања од 600 до 1000 °C. Дифракција рендгенских зрака на праху (XRD) је коришћена за праћење еволуције фазног састава синтетисаних и синтерованих узорака. Морфологија синтероване керамике испитивана је скенирајућом електронском микроскопијом (CEM), а вибрацион траке одабраних спектра су испитане ФТИР методом. Згушњавање и еволуција микроструктуре су одређене коришћењем релативне геометријске густине одабраних узорака. Приказани су најповољнији услови за добијање високотемпературног керамичког материјала на бази Ce, Sr фосфата.*

Кључне речи*: Монацит, стронцијум, синтеровање, рендгенска дифракција, CEM.*